Accepted Manuscript

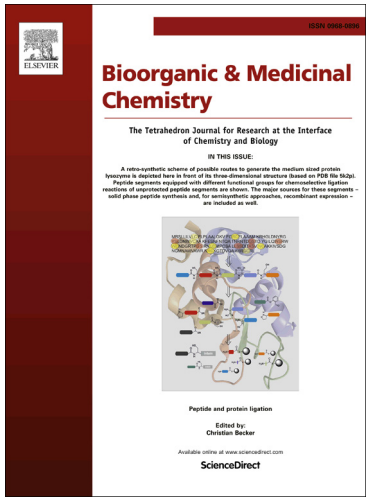

9-Substituted acridine derivatives as acetylcholinesterase and butyrylcholinesterase inhibitors possessing antioxidant activity for Alzheimer's disease treatment

Galina F. Makhaeva, Sofya V. Lushchekina, Natalia P. Boltneva, Olga G. Serebryakova, Elena V. Rudakova, Alexey A. Ustyugov, Sergey O. Bachurin, Alexander V. Shchepochkin, Oleg N. Chupakhin, Valery N. Charushin, Rudy J. Richardson

PII: S0968-0896(17)31509-2
DOI: http://dx.doi.org/10.1016/j.bmc.2017.09.028
Reference: BMC 13988

To appear in: *Bioorganic & Medicinal Chemistry*

Received Date: 24 July 2017
Revised Date: 17 September 2017
Accepted Date: 18 September 2017

Please cite this article as: Makhaeva, G.F., Lushchekina, S.V., Boltneva, N.P., Serebryakova, O.G., Rudakova, E.V., Ustyugov, A.A., Bachurin, S.O., Shchepochkin, A.V., Chupakhin, O.N., Charushin, V.N., Richardson, R.J., 9-Substituted acridine derivatives as acetylcholinesterase and butyrylcholinesterase inhibitors possessing antioxidant activity for Alzheimer's disease treatment, *Bioorganic & Medicinal Chemistry* (2017), doi: http://dx.doi.org/10.1016/j.bmc.2017.09.028

9-Substituted acridine derivatives as acetylcholinesterase and butyrylcholinesterase inhibitors possessing antioxidant activity for Alzheimer's disease treatment

Galina F. Makhaeva[a], Sofya V. Lushchekina[a,b], Natalia P. Boltneva[a], Olga G. Serebryakova[a], Elena V. Rudakova[a], Alexey A. Ustyugov[a], Sergey O. Bachurin[a], Alexander V. Shchepochkin[c,d], Oleg N. Chupakhin[c,d], Valery N. Charushin[c,d], Rudy J. Richardson[e,f]

[a]*Institute of Physiologically Active Compounds Russian Academy of Sciences, Chernogolovka, 142432, Russia*

[b]*Emanuel Institute of Biochemical Physics Russian Academy of Sciences, Moscow, 119334, Russia*

[c]*Institute of Organic Synthesis of the Russian Academy of Sciences, S. Kovalevskaya Str., 22, Ekaterinburg, 620041, Russia.*

[d]*Ural Federal University, Mira St. 19, Ekaterinburg, 620002, Russia*

[e]*Department of Environmental Health Sciences, University of Michigan, Ann Arbor, MI 48109 USA*

[f]*Department of Neurology, University of Michigan, Ann Arbor, MI 48109 USA*

*Corresponding author:

Dr. Rudy J. Richardson
Computational Toxicology Laboratory
Toxicology Program
Department of Environmental Health Sciences
University of Michigan
Ann Arbor, Michigan 48109-2029 USA

E-mail: rjrich@umich.edu
Tel: +1-734-936-0769
Fax: +1-734-763-8095

Abstract

We investigated the inhibitory activity of 4 groups of novel acridine derivatives against acetylcholinesterase (AChE), butyrylcholinesterase (BChE) and carboxylesterase (CaE) using the methods of enzyme kinetics and molecular docking. Antioxidant activity of the compounds was determined using the 2,2'-azinobis-(3-ethylbenzothiazoline-6-sulfonic acid) ($ABTS^{\cdot+}$) radical decolorization assay as their ability to scavenge free radicals. Analysis of the esterase profiles and antiradical activities of the acridine derivatives showed that 9-aryl(heteroaryl)-N-methyl-9,10-dihydroacridines have a high radical-scavenging activity but low potency as AChE and BChE inhibitors, whereas 9-aryl(heteroaryl)-N-methyl-acridinium tetrafluoroborates effectively inhibit cholinesterases but do not exhibit antiradical activity. In contrast, a group of derivatives of 9-heterocyclic amino-N-methyl-9,10-dihydroacridine has been found that combine effective inhibition of AChE and BChE with rather high radical-scavenging activity. The results of molecular docking well explain the observed features in the efficacy, selectivity, and mechanism of cholinesterase inhibition by the acridine derivatives. Thus, in a series of acridine derivatives we have found compounds possessing dual properties of effective and selective cholinesterase inhibition together with free radical scavenging, which makes promising the use of the acridine scaffold to create multifunctional drugs for the therapy of neurodegenerative diseases.

Keywords

9-heterocyclic amino-N-methyl-9,10-dihydroacridines; esterase profile; acetylcholinesterase inhibitors; butyrylcholinesterase inhibitors; molecular docking; antioxidant activity

1. Introduction

Acridines are considered privileged scaffolds in drug discovery for protozoan and neurodegenerative diseases [1]. Acridine derivatives have a broad spectrum of therapeutic applications as antibacterial [2], antimalarial [3], antileishmanial and antitrypanosomal [4], antiviral [5], anticancer [6] and antiprion [7-9] agents. They have also been reported to have anti-inflammatory, anti-diabetic [10, 11] and anti-Alzheimer activity [12-14]. Recently they demonstrated an anti-TDP-43 aggregation effect in ALS disease models [15]. Acridine derivatives are optimal starting points for the design of novel hybrid and dimeric multitarget lead and drug candidates [1].

Alzheimer's disease (AD), the most widely encountered type of dementia in older people, is a multifactorial and fatal neurodegenerative disorder, which is characterized by an inexorable decline in cognitive function and memory that progresses to the complete degradation of personality. AD involves degeneration of cholinergic neurons and diminishing cholinergic transmission [16]. Anticholinesterase drugs are used to compensate for deficiency of the neurotransmitter acetylcholine [17]. They replenish the acetylcholine deficit in the brain by inhibiting cholinesterases, thereby increasing the duration of acetylcholine action on postsynaptic receptors, thus enhancing cholinergic transmission. In a normal brain, acetylcholine is predominantly (80%) hydrolyzed by AChE, whereas BChE plays a supplementary role. However, with progression of AD, the AChE activity decreases, whereas the activity of BChE gradually increases [18, 19]. This phenomenon enhances the significance of BChE as an additional therapeutic target for reducing the cholinergic deficiency inherent in AD [20-22].

Currently, AD therapy is mainly founded on cholinesterase inhibitors, which are able to increase acetylcholine levels in cholinergic synapses. To date, the number of approved drugs is limited to only three cholinesterase inhibitors (rivastigmine, donepezil, and galantamine), and the N-methyl-D-aspartate (NMDA) receptor antagonist, memantine [23, 24].

The multifactorial nature of AD is commonly recognized, implying the involvement a number of neurobiological targets in the development of this neurodegenerative disease. In this context, the concept of multitarget drugs having an integrated action on a number of biological targets involved in pathogenesis of the disease currently appears to be highly promising in the design of drugs for treating AD [25, 26].

Oxidative stress leading to oxidative damage of cell membranes, mitochondria, lipids and proteins, may be one of the possible causes of neuronal death [27]. Oxidative stress is characterized

as an imbalance between biochemical processes leading to the production of reactive oxygen species (ROS) and their removal [28]. The efficiency of the brain's antioxidant system gradually declines with age, and this decline is more pronounced in AD patients. This fact substantiates the use of antioxidants in AD therapy [29], and the development of cholinesterase inhibitors with attendant antioxidant properties is a modern trend in research directed toward efficient therapy of AD [30-32].

It is well known that compounds of the acridine family are able to inhibit AChE and BChE [33, 34, 35]. Tacrine (9-amino-1,2,3,4-tetrahydroacridine), a potent reversible inhibitor of AChE and BChE, was the first drug approved by the FDA for treatment of Alzheimer's disease [36]. However, it was withdrawn from clinical use because of its hepatotoxicity [37]. Nevertheless, there is a continuing interest in the tacrine template to design new hybrid molecules that might be safer and more effective AD drugs than tacrine [38-41]. Although the precise mechanism of hepatotoxicity of tacrine has not been elucidated, oxidative stress appears to be involved to some degree. Therefore, derivatization of acridine-based anticholinesterase compounds in a manner that confers antioxidant activity would be expected to ameliorate this toxic concern.

The aim of the present study was to investigate the inhibitory properties of novel acridine derivatives against the key enzymes of the cholinergic nervous system AChE and BChE, using both kinetic and computational molecular modeling methods, as well to assess the ability of compounds to scavenge free radicals using the 2,2'-azino-bis(3-ethylbenzothiazoline-6-sulphonic acid) (ABTS) assay. In addition, we have determined the inhibitory activity of the synthesized acridines toward carboxylesterase (CaE, EC 3.1.1.1), a serine hydrolase structurally related to cholinesterases that catalyzes the hydrolysis of many therapeutically important agents bearing ester and other hydrolysable groups [42, 43]. The ability of anticholinesterase compounds used for AD therapy to inhibit CaE could lead to undesirable drug-drug interactions [44]. Consequently, in this investigation we were seeking to find compounds with anticholinesterase and antiradical activity but lacking anti-CaE activity.

2. Results and discussion

2.1. Synthesis of acridine derivatives

Acridine derivatives can be obtained using three main approaches. The first one is based on construction of the acridine ring system through the reaction of the corresponding carboxylic acid with diphenylamine in the presence of $ZnCl_2$ at elevated temperatures (200-260 ^oC) [45, 46] The second approach entails functionalization of acridine using metal-catalyzed cross-coupling reactions [47]. However, these two methods have some disadvantages, such as the necessity to incorporate good leaving groups, the formation of byproducts due to side reactions of organometallic reagents, and some difficulties in eliminating catalysts and auxiliary ligands. Fortunately, there is a third approach involving metal-free methods for direct C-H functionalization of acridines, based on nucleophilic aromatic substitution of hydrogen, the so-called S_N^H reactions [48-54].

A mechanism that is commonly accepted for the S_N^H reactions involves two steps. The first one is addition of a nucleophile to an aromatic ring, thus leading to the formation of σ^H-adducts. Oxidative aromatization of σ^H-adducts is realized at the second step by action of an outer-sphere oxidant (**Scheme 1**). The ability of σ^H-adducts to undergo aromatization into S_N^H products varies greatly: from very unstable and hardly spectroscopically detectable σ^H-adducts to rather stable compounds, derived from the reactions of N-methylacridinium salts. In the latter case, dihydroacridines can be easily isolated for studying their biological activity. Moreover, it is possible to carry out aromatization of dihydroacridines in order to estimate how these structural changes affect their biological properties.

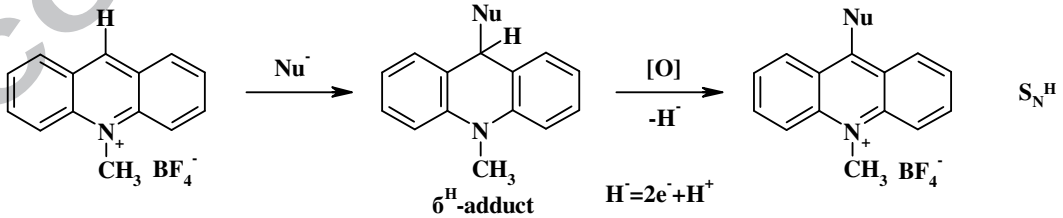

Scheme 1. Mechanism of S_N^H reactions.

Chemical structures of the studied compounds are given in **Fig.1.** All compounds can be classified into 4 groups, depending on the structure of the core acridine nucleus and substituents

in the 9-position: 9-Aryl-N-methyl-9,10-dihydroacridines (compounds **1a-j**), 9-Aryl-N-methylacridinium tetrafluoroborates (compounds **2a-m**), 9-heterocyclic amino derivatives of 10-methyl-9,10-dihydroacridine (compounds **3a-f**), and 9-amino-N-methyl acridinium tetrafluoroborates (compounds **4a,b).**

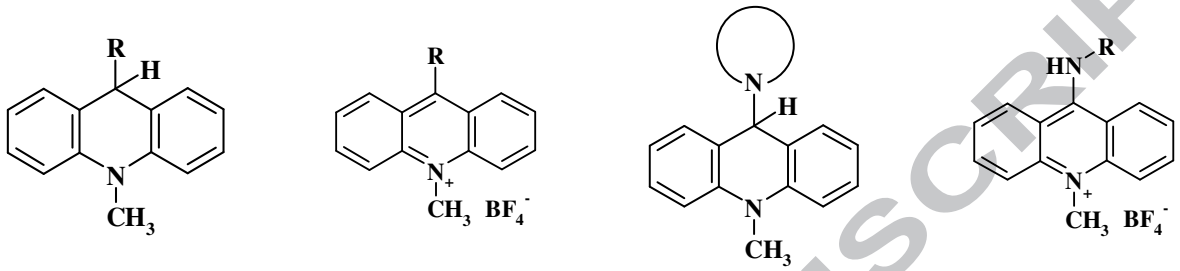

1a-j **2a-m** **3a-f** **4a,b**

Fig. 1. Structures of the studied acridine derivatives.

Synthetic pathways to these compounds have previously been reported [55-57]. Dihydroacridines **1a**,**b**,**f**,**g**,**j** have been prepared through the reaction of 10-methyl-acridinium iodide with the corresponding magnesium aryl bromides. Compounds **1h,i** are derived from the reaction of the 10-methylacridinium ion with sodium phenolates in diethyl ether at room temperature. Aniline proved to react with the acridinium cation in DMSO to form the corresponding amino compound **1c**. Carbamoyl derivatives **1d** and **1e** were obtained by treatment of the amino compound **1c** with the corresponding anhydrides.

Acridinium salts **2a-m** have been obtained by electrochemical oxidation of dihydroacridines according to the previously reported procedure [55]. The reaction of NH-heterocyclic compounds with the 10-methylacridinium ion takes place smoothly in the presence of a base, thus affording the corresponding acridines **3a-f** [56]. Compounds **4a and 4b** have been obtained by electrochemical amination of 10-methylacridinium tetrafluoroborate [58].

2.2. Inhibition of AChE, BChE and CaE. Structure-activity relationships

For all 31 acridine derivatives, we have determined their esterase profiles, i.e., the ability to inhibit several esterases, including AChE, BChE, and CaE. This approach enables one to estimate both the primary pharmacological effects of the tested compounds and their possible

adverse effects [59-63]. AChE from human erythrocytes was used along with two enzymes of non-human origin: equine serum BChE and porcine liver CaE. These sources of BChE and CaE were used because of their relatively low cost, high sequence identity to human enzymes [60, 62], and the exploratory character of this work.

The inhibitory activity against the esterases was characterized as the percentage of control inhibition at 20 μM or as the IC_{50} value, i.e., the inhibitor concentration required to reduce the enzyme activity by 50%. Bis-4-nitrophenyl phosphate (BNPP), which is a selective CaE inhibitor, and tacrine, which is an effective AChE and BChE inhibitor, were used as positive controls in the study of enzyme inhibition. The results of the inhibitory activity of 4 groups of acridine derivatives against AChE, BChE and CaE, characterizing the esterase profile of compounds, are presented in **Table 1.**

Table 1. Esterase profiles and ABTS-radical scavenging activity of acridine derivatives.

Comp.	R	Inhibitory activity against AChE, BChE and CaE IC_{50} ± SEM (μM) or inhibition % at 20 μM			$ABTS^{\bullet+}$ scavenging	
		AChE	**BChE**	**CaE**	**TEAC***	**IC_{50} ± SEM (μM)**
		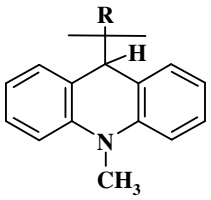				
		9-Aryl-N-methyl-9,10-dihydroacridines				
1a	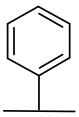	n.a	62.1±6.7	n.a	1.02	18.9±1.5
1b	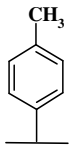	> 20 (5.1±0.9%)	> 20 (10.6±2.1%)	n.a.	0.93	22.4±1.6
1c	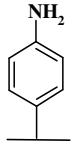	n.a.	66.5±5.9	n.a.	0.97	19.6±1.5
1d	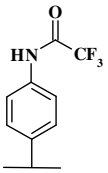	n.a.	> 20 (7.1±1.3%)	n.a.	0.91	21.05±1.6
1e	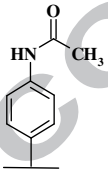	n.a.	> 20 (10.8±1.9%)	> 20 (7.2±1.3%)	0.99	20.3±1.4
1f	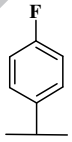	n.a.	> 20 (11.1±1.9%)	n.a.	0.89	24.7±1.5
1g	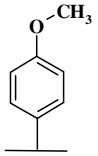	> 20 (9.3±1.8%)	> 20 (11.6±2.1%)	n.a.	0.95	20.4±1.3

1h	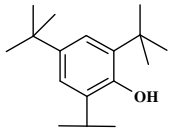	n.a.	> 20 (13.4±2.2%)	n.a.	0.88	23.2±1.9
1i	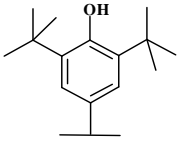	n.a.	> 20 (10.4±1.9%)	> 20 (23.6±3.3%)	1.0	19.6±1.1
1j		n.a.	> 20 (12.3±2.2%)	> 20 (11.1±2.1%)	0.92	22.9±1.5

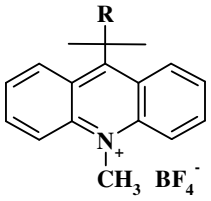

9-Aryl-N-methylacridinium tetrafluoroborates

2a	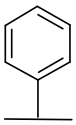	61.3±5.5	51.9±5.7	> 20 (22.6±2.9%)	0.03	n.d.
2b	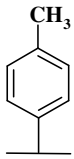	41.5±3.3	40.7±4.3	> 20 (16.3±2.9%)	0.03	n.d.
2c	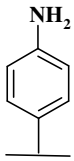	7.62±0.69	39.1±4.3	> 20 (18.6±3.1%)	0.14	n.d.
2d	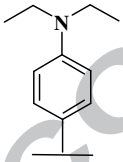	25.2±2.3	3.35±0.34	n.a.	0.04	n.d.
2e	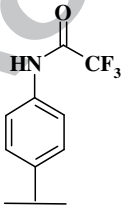	36.5±2.9	> 20 (7.7±1.3%)	> 20 (7.2±1.4%)	0.02	n.d.

2f	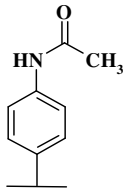	54.3±4.8	35.1±2.9	n.a.	0.03	n.d.
2g	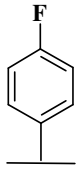	32.3±2.9	> 20 (8.2±1.5%)	> 20 (5.9±1.1%)	0.03	n.d.
2h	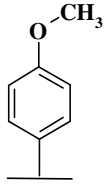	13.7±1.2	58.5±5.7	> 20 (7.8±1.4%)	0.02	n.d.
2i	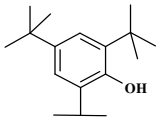	> 20 (16.7±2.0%)	2.74±0.24	> 20 (31.2±2.8%)	0.37	n.d.
2j	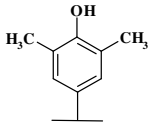	49.8±3.9	61.8±6.6	n.a.	0.43	n.d.
2k	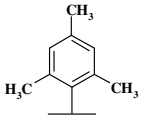	60.1±5.4	> 20 (14.2±2.5%)	n.a.	0.01	n.d.
2l	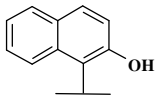	> 20 (7.3±1.3%)	50.8±4.5	> 20 (8.9±1.6%)	0.03	n.d.
2m	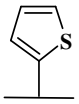	40.9±4.3	58.3±5.2	> 20 (6.1±1.1%)	n.a.	n.d.

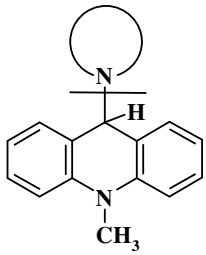

9-Heterocyclic amino derivatives of N-methyl-9,10-dihydroacridine

3a	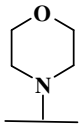	12.3±1.1	0.46±0.05	> 20 (16.4±1.8%)	0.83	25.6±1.9

3b	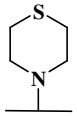	11.8±0.6	0.84±0.05	> 20 (5.0±0.9%)	0.74	29.7±2.1
3c	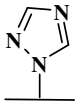	18.8±1.1	0.81±0.09	> 20 (5.4±1.0%)	0.65	36.5±2.8
3d	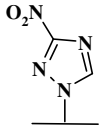	16.7±1.3	1.17±0.09	> 20 (10.6±1.8%)	0.50	47.2±3.2
3e	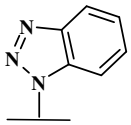	12.4±1.3	1.08 ±0.09	> 20 (15.3±1.8%)	0.59	40.6±2.4
3f	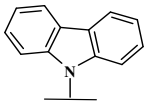	> 20 (5.6±0.9%)	13.0±1.2	n.a.	0.80	27.0±1.2

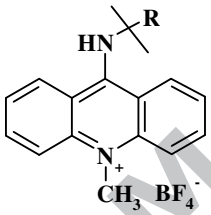

9-Amino-N-methylacridinium tetrafluoroborates

4a	H	39.5±3.5	4.83±0.39	n.a.	0.09	n.d.
4b	*n*-Bu	> 20 (16.8±1.7)%	15.7±1.5	n.a.	0.05	n.d.
	Tacrine	0.60±0.05	0.0290±0.0002	n.a.	n.d.	n.d.
	BNPP	n.a.	n.a.	1.80±0.11	n.d.	n.d.
	Trolox	n.d.	n.d.	n.d.	1.0	21.6±1.4

Esterase profiles: n.a. – not active at 20 μM.
Values expressed as % correspond to % inhibition at 20 μM.
Values without units of measurement correspond to IC_{50} values in μM.
$ABTS^{\cdot+}$- scavenging activity: TEAC values are expressed as Trolox equivalents calculated from $(A_0–A_{test})/(A_0–A_{Trolox})$ at 20 μM concentrations, where A_0 is the absorbance of a control lacking any radical scavenger, A_{test} and A_{Trolox} are the absorbances of the remaining $ABTS^{\cdot+}$ in the presence of the test compound or Trolox, respectively. IC_{50} values (compound concentration required for 50 % reduction of ABTS-radical) were determined for the most active compounds.
n.d. = not determined
n.a. = no activity

It follows from the data given in **Table 1** that compounds of the first group, derivatives of 9-aryl-N-methyl-9,10-dihydroacridines **1a-j** (aryl substituent at C-9 and uncharged nitrogen atom in the ring), proved to be only slight inhibitors of the cholinesterases.

It is worth noting that their structural aromatic analogues, 9-aryl(hetaryl)-N-methylacridinium tetrafluoroborates (group 2), which carry a positive charge, demonstrated higher anticholinesterase activity: compare compounds **1b** and **2b, 1c** and **2c, 1d** and **2e, 1e** and **2f, 1f** and **2g, 1g** and **2h, 1h** and **2i.** The activity and selectivity of these compounds toward AChE and BChE depended on the structure of the 9-aryl substituents. The presence of a nitrogen atom in the *para*-position of the aryl substituent (compounds **2c** and **2d)** facilitated inhibitory activity against both enzymes**.** In addition, the high anti-BChE activity of compound **2i** is noteworthy.

Compounds of the third group, namely derivatives of 9-heterocyclic amino-N-methyl-9,10-dihydroacridine (compounds **3a-f**), appeared to be the most promising inhibitors of cholinesterases. These compounds were moderate inhibitors of AChE (IC_{50} values are about 10^{-5} M), while they more effectively inhibited BChE with IC_{50} values in the range of 10^{-6} – 10^{-7} M. Compounds of this series were more selective toward BChE in comparison with AChE; namely, 9-morpholino (**3a**), 9-thiomorpholino (**3b**) and 9-(1,2,4-triazolyl) (**3c**) substituted dihydroacridines were the best BChE inhibitors with IC_{50} values of 0.46±0.05, 0.84±0.05 and 0.81±0.09 μM, respectively.

Derivatives of 9-amino-N-methyl-9,10-dihydroacridinium tetrafluoroborate, compounds **4a** and **4b**, were also found to be more effective inhibitors of BChE relative to AChE.

2.3. Kinetic studies of AChE and BChE inhibition

Detailed kinetic studies of cholinesterase inhibition with the most active acridine derivatives demonstrated that these compounds are predominantly reversible inhibitors of the mixed type (**Table 2**). It is interesting to note that the mechanism of inhibiting AChE switched from mixed to competitive when the morpholino substituent in compound **3a (Fig. 2A**) was replaced with the thiomorpholino analogue **3b (Fig. 3A**). In contrast, only a mixed mechanism was exhibited by both compounds for inhibiting BChE (**Fig. 2B and 3B).** The same situation was observed for the pair of compounds with 1,2,3-benzotriazolyl (**3e**) and 1,2,4-triazolyl (**3c**) substituents (**Table 2**).

Table 2. Inhibition constants for active acridine derivatives toward AChE and BChE [a].

Comp.	R	AChE		BChE	
		K_i (μM)	αK_i (μM)	K_i (μM)	αK_i (μM)
2c	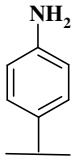	2.66±0.24	8.95 ± 0.91	19.0± 1.7	55.4 ± 4.9
2d	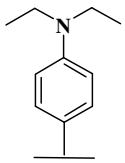	13.2±1.4	28.0±2.5	0.94 ± 0.08	4.22 ± 0.34
2i	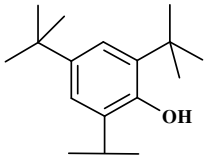	n.d.	n.d.	1.46±0.15	4.75±0.42
3a	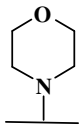	4.01±0.36	19.6 ± 1.6	0.41 ± 0.03	1.17 ± 0.11
3b	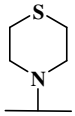	3.75±0.33	n.a.	0.35 ± 0.03	1.31 ± 0.14
3c	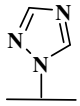	3.34±0.31	n.a.	0.16±0.02	0.72±0.06
3e	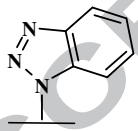	6.43±0.57	17.9±1.6	0.49 ± 0.04	2.13 ± 0.23

[a] Values for K_i (competitive inhibition constant) and αK_i (non-competitive inhibition constant) were determined from analysis of slopes of 1/V versus 1/S at various inhibitor concentrations. The values (mean ± SEM) were taken from at least three experiments.
n.d. = not determined.
n.a. = not applicable. These compounds were competitive inhibitors of AChE; therefore, only K_i applies.

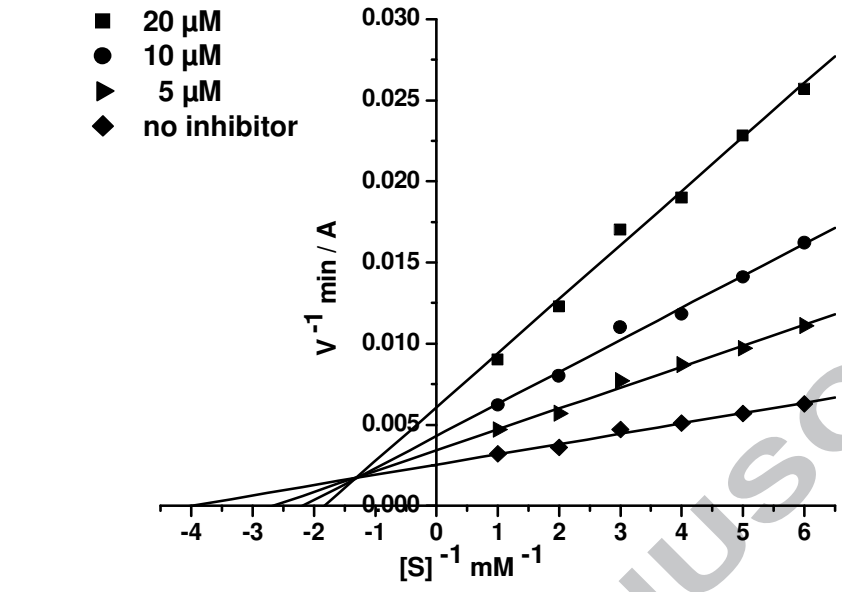

A

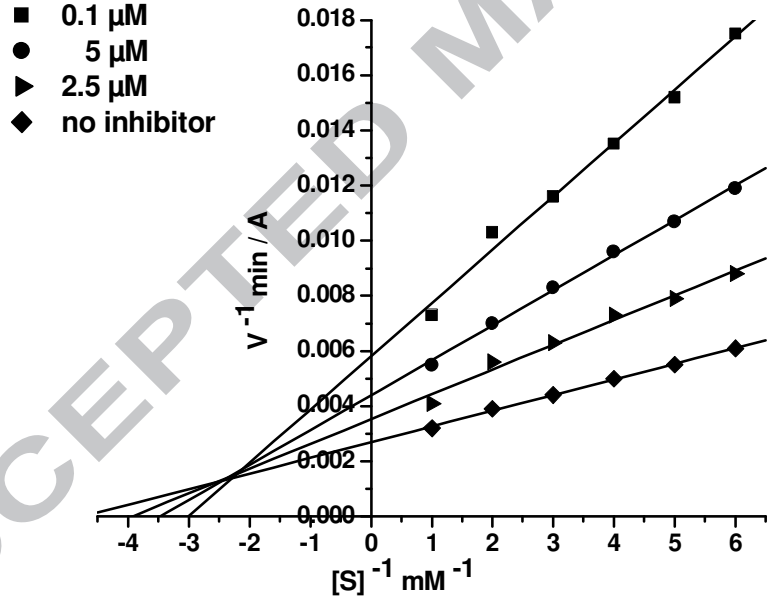

B

Fig. 2. Steady state inhibition of AChE (**A**) and BChE (**B**) by compound **3a**. Lineweaver-Burk double-reciprocal plots of initial velocity and substrate concentrations in the presence of inhibitor **3a** (three concentrations) and without inhibitor are presented. Plots **A** and **B** show mixed-type inhibition.

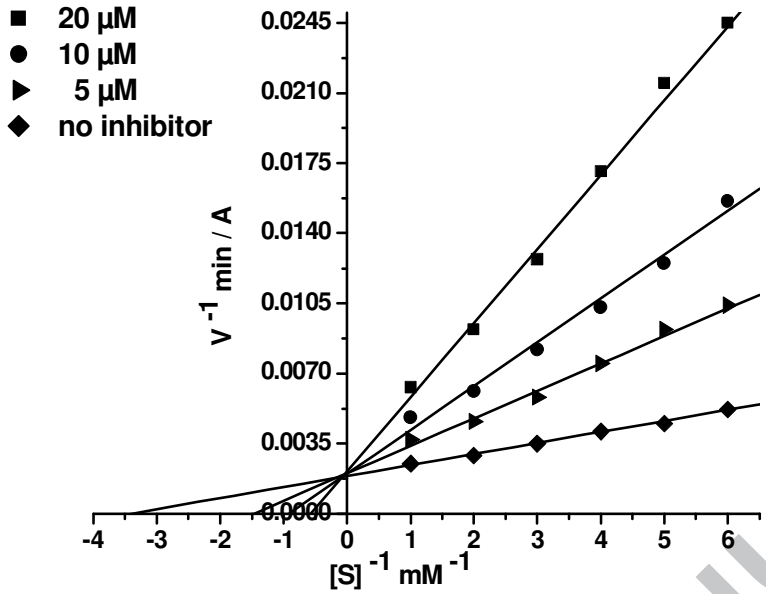

A

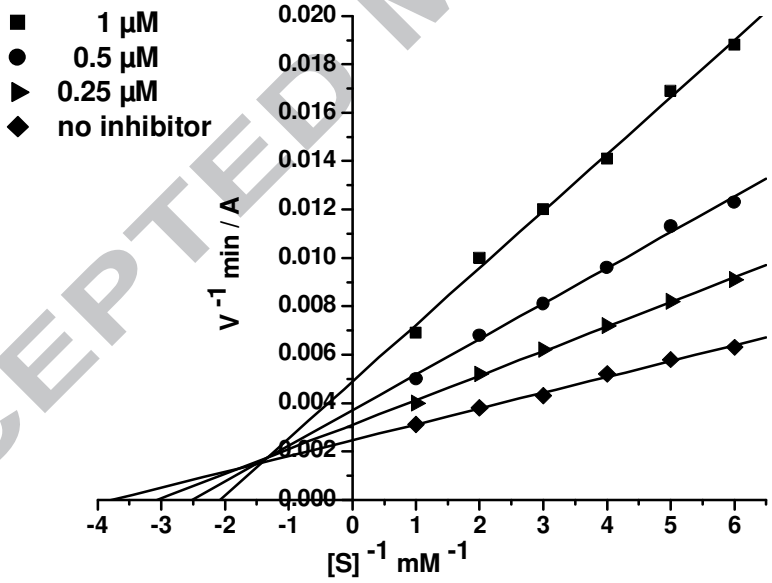

B

Fig. 3. Steady state inhibition of AChE (**A**) and BChE (**B**) by compound **3b**. Lineweaver-Burk double-reciprocal plots of initial velocity and substrate concentrations in the presence of inhibitor **3b** (three concentrations) and without inhibitor are presented. Plot **A** shows competitive inhibition and plot **B** exhibits mixed-type inhibition.

2.4. Molecular modeling studies

To explain the varied efficacy of the studied acridine derivatives toward cholinesterases and to elucidate their inhibitory mechanism, molecular docking studies were carried out for all compounds as ligands with AChE and BChE as receptors.

Quantum-chemical optimization of these compounds revealed differences in geometries between dihydroacridine and acridinium derivatives, which have a conjugated π-system and positive charge (**Fig. 4**). In spite of conjugation between the aryl substituent and the acridinium moiety, these molecules are not fully planar due to steric conflicts between the acridine ring system and benzene rings, though they are aligned along one axis. Dihydroacridine derivatives have a sp^3-hybridized carbon atom that determines the bend in their structure. The results of quantum-chemical optimization were well correlated with experimental X-ray diffraction data [55].

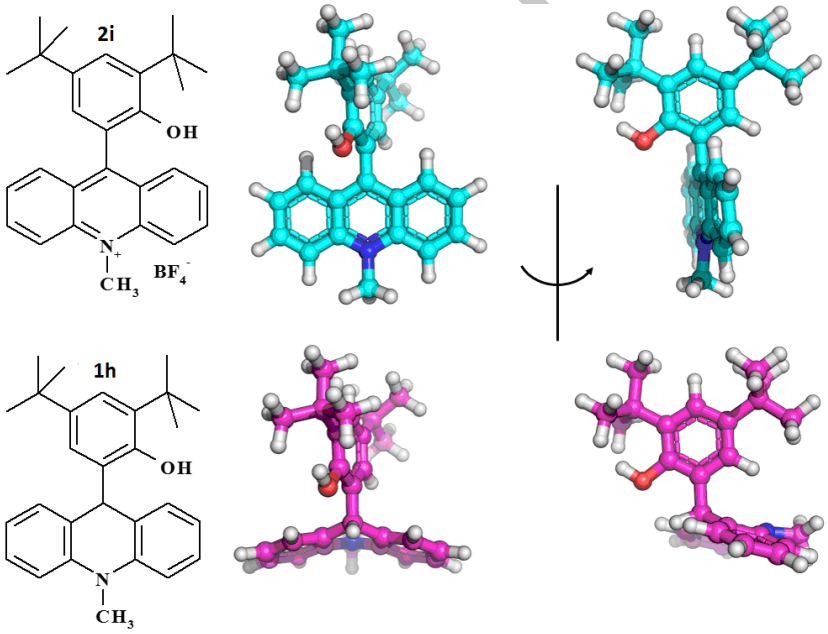

Fig. 4. Geometries of acridinium (upper) and dihydroacridine compounds (lower) rows. Atom colors: carbon = cyan (upper row) or magenta (lower row); nitrogen = blue; oxygen = red; hydrogen = white. The C-9 atom is sp^3-hybridized in compound **1h**, but due to the symmetry of the dihydroacridine fragment, compound **1h** does not have enantiomers. The C-9 atom in compound **2i** is sp^2-hybridized. The different hybridization of this atom in compounds **2i** and **1h** determines the dissimilar configurations of these ligands.

Results of molecular docking revealed that some compounds can nearly reach the bottom of the active site gorge of cholinesterases (catalytic active site, CAS), AChE or BChE, while others bind at the peripheral anionic site (PAS), or at both CAS and PAS, thus explaining differences in the mode of inhibition and selectivity of these compounds. As typically seen for cholinesterases, positively charged ligands generally show better inhibitory activity compared to uncharged analogues [64]. For compounds that bind at the bottom of the gorge, a positive charge on the acridinium fragment (or the N-protonated piperidine moiety in dihydroacridines) plays an important role in binding due to cationic π-interactions with Trp86(82) and charge-pairing with Glu202(197), where the first number refers to the AChE sequence and the second number in parentheses refers to the BChE sequence. As an example, both compounds **1h** and **2i** bind at the active site of BChE, but the absence of positively charged groups in **1h**, like in other 9-aryl-9,10-dihydro-N-methylacridines, lessens their computed binding affinity and experimentally measured inhibitory activity (**Fig. 5**).

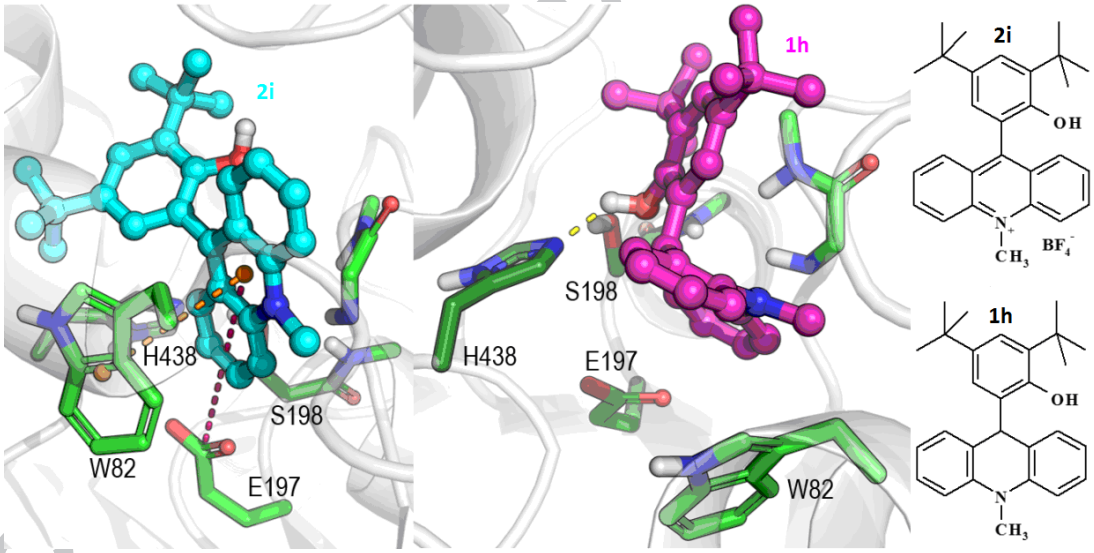

Fig. 5. Binding modes for the acridinium salt **2i** (left; cyan carbons) and dihydroacridine **1h** (right; magenta carbons) at the bottom of the BChE gorge. The structural formulae of **2i** and **1h** are shown on the far right. Active site amino acid residues: carbon = green; nitrogen = blue; oxygen = red; hydrogen = white; for clarity, some hydrogens are not shown. Secondary structures of BChE are shown in white and gray in the background. Dashed lines depict cationic π-interaction with Trp82 and charge-pairing with Glu197 for the **2i** ligand.

Due to the presence of aromatic fragments at the PAS of AChE, a positive charge in the ligand molecule is also important, given that it contributes to binding, although this effect is not greatly pronounced. Both compounds **2h** and **1g** bind at the PAS of AChE (**Fig. 6**) and the positive charge of **2h** has π-cation interactions with Trp286, thus resulting in a slightly better inhibitory activity compared to that of **1g.**

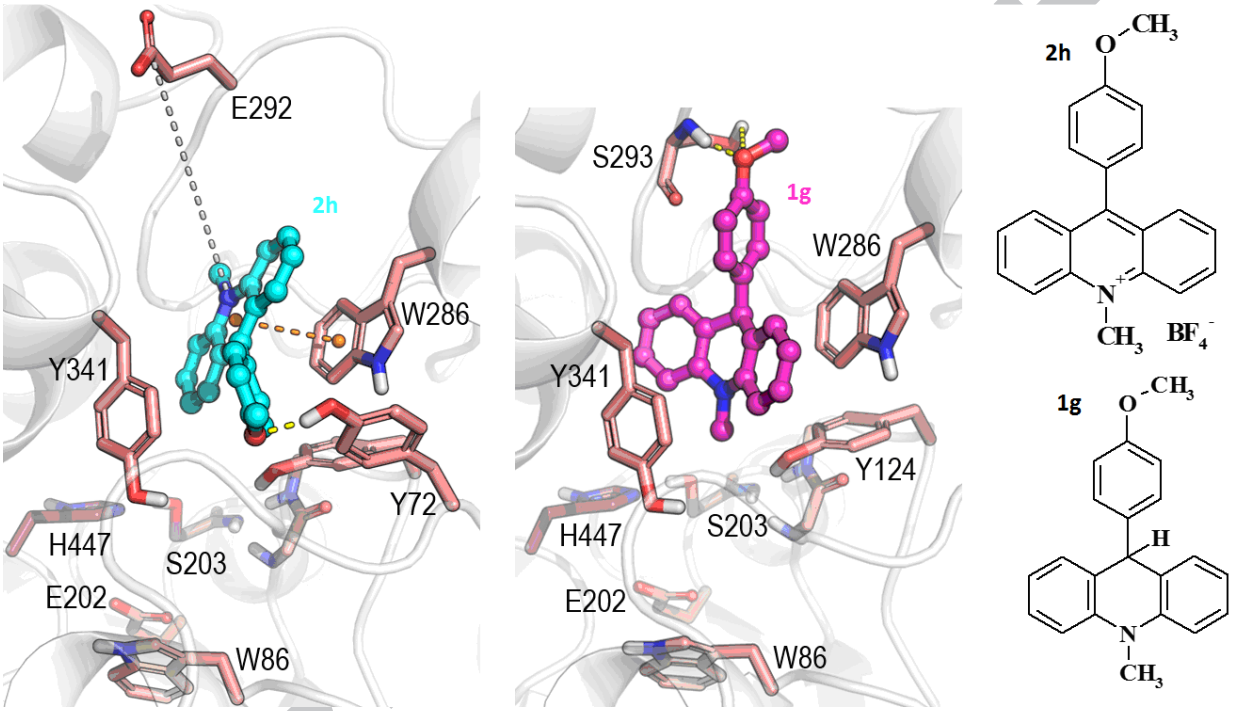

Fig. 6. Binding modes for the acridinium salt **2h** (left; cyan carbons) and dihydroacridine **1g** (right; magenta carbons) at the PAS of AChE. White dashes show possible contacts due to conformational change and protein accommodation, as has been shown previously in molecular dynamics studies for positively charged compounds binding at the AChE PAS [65]. Interacting amino acid residues are shown with carbon = tan; nitrogen = blue; hydrogen = white; some hydrogens are not shown to enhance clarity. Structural formulae of **2h** and **1g** are shown on the far right.

Some compounds can reach the bottom of the wider gorge found in BChE, but not the narrower gorge found in AChE, as shown for compound **2i**, which contains bulky *tert*-butyl groups (**Fig. 7**).

When the size of substituents in the acridinium ring allows these compounds to reach the bottom of the AChE gorge, tighter and more specific interactions provide a higher inhibitory activity toward AChE rather than BChE, as observed for compound **2c** (**Fig. 8**).

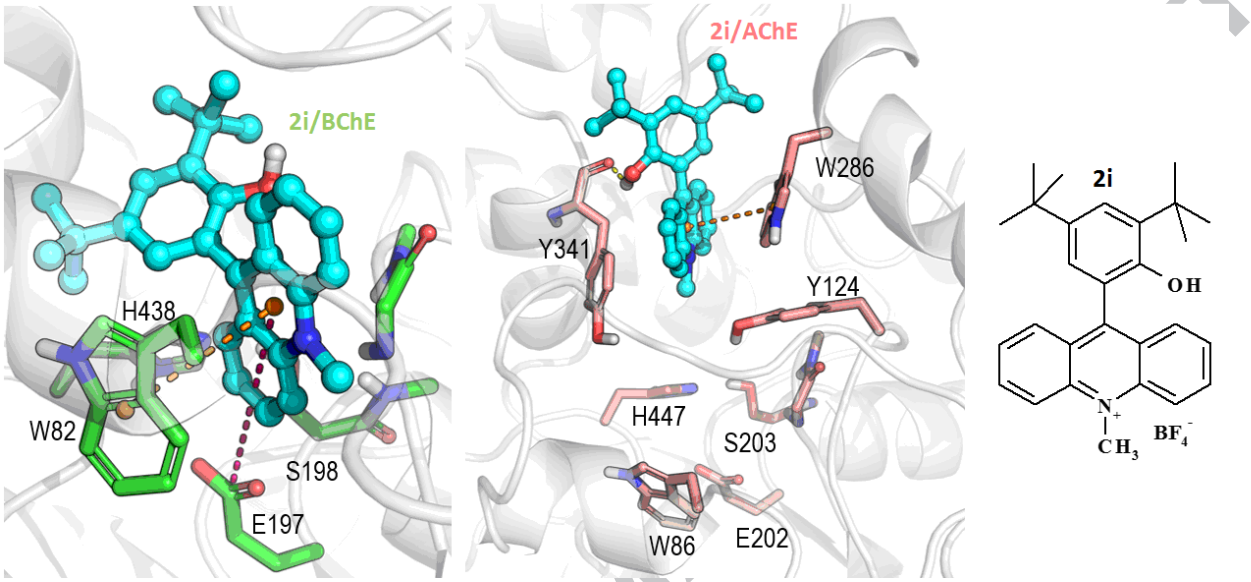

Fig. 7. Binding positions of compound **2i** in the active site of BChE (left; cyan carbons; amino acid residues shown with carbon = green; nitrogen = blue; oxygen = red; hydrogen = white; some hydrogens not shown for clarity) and at the PAS of AChE (right; cyan carbons; amino acid residues shown with carbon = tan; nitrogen = blue; oxygen = red; hydrogen = white; some hydrogens not shown for clarity). Dashed lines depict cationic π-interaction with Trp82 and charge-pairing with Glu197 for the **2i** ligand in BChE and cationic π-interaction with Tryp286 in AChE. Background shows secondary structure of protein in white and gray ribbon view. The structural formula of **2i** is shown on the far right.

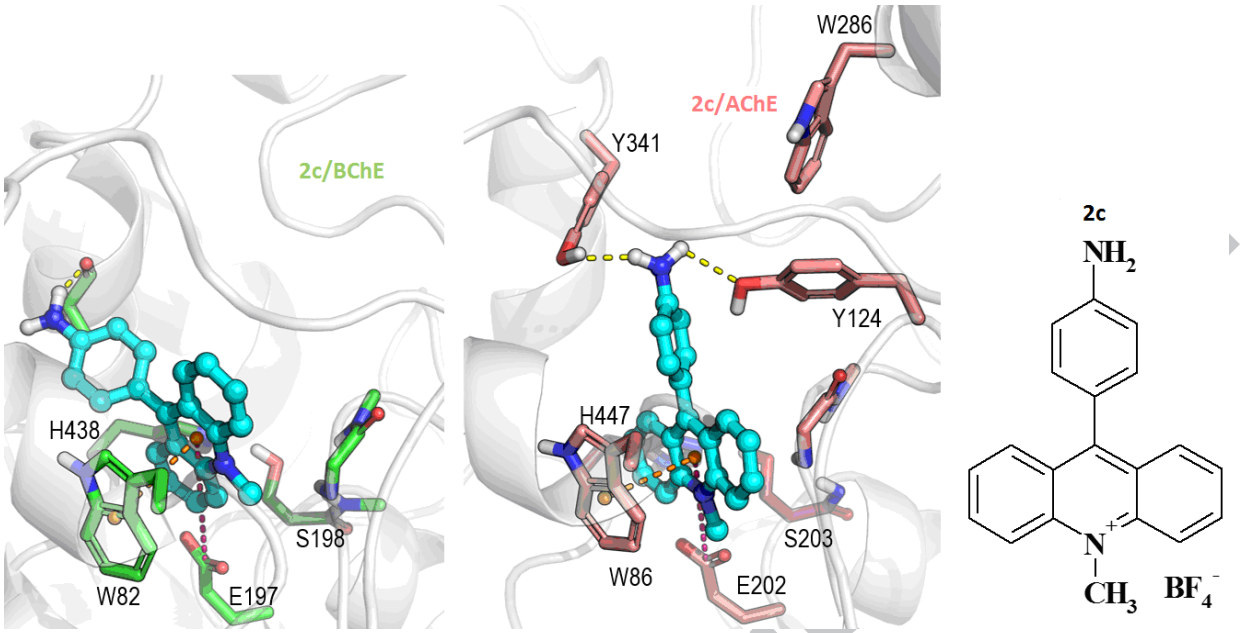

Fig. 8. Binding positions of compound **2c** in the active site of BChE (left; cyan carbons; amino acid residues shown with carbon = green; nitrogen = blue; oxygen = red; hydrogen = white; some hydrogens not shown for clarity) and AChE (right; cyan carbons; amino acid residues shown with carbon = green; nitrogen = blue; oxygen = red; hydrogen = white; some hydrogens not shown for clarity). The ligand has a few more specific interactions with AChE amino acid residues than it does with BChE, resulting in a slightly higher computed binding affinity and experimental inhibitory activity toward AChE (**Table 1**). Dashed lines depict cationic π-interactions, charge-pairing, and hydrogen bonds. Background shows secondary structure of protein in white and gray ribbon view. The structural formula of **2c** is shown on the far right.

Although dihydroacridines are generally less active than acridinium derivatives as cholinesterase inhibitors due to the absence of a positive charge in the dihydroacridines, their amino derivatives (9-heterocyclic amino-N-methyl-9,10-dihydroacridines) have enhanced activity due to the presence of a tertiary nitrogen atom, which can be protonated (calculated pK_a ~7-8), thus providing more specific interactions. Additionally, these specific interactions might mediate the change in mechanism of inhibition (i.e., mixed-type vs. competitive), as exemplified by compounds **3a** and **3b**). As shown in **Fig. 9**, compound **3b** has a calculated pK_a of 7.86, and its docking poses reside in the AChE active site. In contrast, compound **3a** has a computed pK_a of 6.65, and its docking poses occupy both the active site and the PAS of AChE.

2.5. Antioxidant activity of acridine derivatives

Antioxidant activity of compounds was determined using the 2,2'-azinobis-(3-ethylbenzothiazoline-6-sulfonic acid) ($ABTS^{\bullet+}$) radical decolorization assay [66] as their ability to scavenge free radicals. Here, antioxidant activity is reported as Trolox equivalent antioxidant capacity (TEAC) values by comparing (A_0–A_{test}) of a test compound with (A_0–A_{Trolox}) of the Trolox standard after 1 h of reaction time, where A_0 is the absorbance of a control lacking any radical scavenger, and A_{test} and A_{Trolox} are the absorbances of the remaining $ABTS^{\cdot+}$ in the presence of the test compound or Trolox, respectively. For the most active compounds, we also determined IC_{50} values (compound concentration required for 50% reduction of the ABTS radical). Lower IC_{50} values are indicative of higher ABTS free radical scavenging ability. The results are presented in **Table 1**.

It follows from the data given in **Table 1** that derivatives of 9-aryl-9,10-dihydro-N-methyl-acridines (group 1) bind $ABTS^{\bullet+}$ most effectively relative to other acridine derivatives. All representatives of this group of compounds (**1a-j**) exhibit a high antiradical activity, which is compared with the standard antioxidant, Trolox.

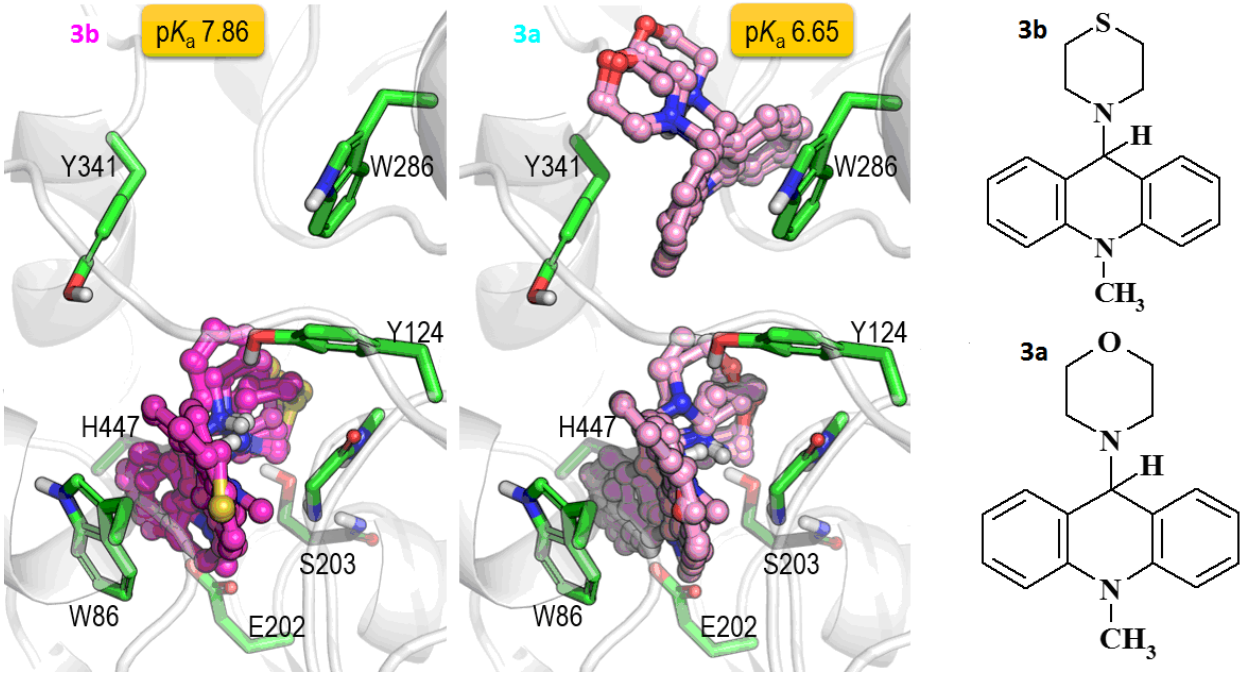

Fig. 9. Docked poses from one docking run for compounds **3b** (right; pink carbons) and **3a** (left; magenta carbons) with AChE (amino acid residues shown with carbon = green; nitrogen = blue; oxygen = red; hydrogen = white; some hydrogens not shown for clarity; secondary structures shown in background as white and gray ribbon). Structural formulae of **3b** and **3a** are shown on the far right.

In contrast, the corresponding charged analogues (group 2), 9-aryl(hetaryl)-N-methyl-acridinium tetrafluoroborates **2a-m**, exhibit very low antiradical activity. The moderate activity of two of these compounds, **2i** and **2j,** may be due to the phenolic R' moieties, which are structures known to have antioxidant properties [66].

Compounds of the third group, derivatives of 9-heterocyclic amino-N-methyl-9,10-dihydroacridine **3a-f**, exhibit good $ABTS^{\bullet+}$ scavenging activity, although their potencies are somewhat lower than that of Trolox ($0.6 < TEAC < 1$). Leaders in this group were compounds **3a** and **3f**.

9-Amino-N-methylacridinium tetrafluoroborates (group 4), compounds **4a** and **4b**, as well as charged 9-aryl(hetaryl)-N-methyl-acridinium tetrafluoroborates (group 2), proved not to bind the $ABTS^{\bullet+}$ radical.

Using the ABTS assay, we evaluated the intrinsic property of compounds to bind free radicals as a "primary antioxidant", i.e., those which actively inhibit oxidation reactions [67, 68]. The $ABTS^{\bullet+}$ indicator radical may be neutralized either by direct reduction via single electron transfer (SET reaction) or by radical quenching via hydrogen atom transfer (HAT), both of which are applicable to the antioxidant action of dihydroacridines. During the process of their oxidation, these compounds transiently form free radicals, which would be capable of binding the $ABTS^{\bullet+}$ radical [69, 70]. These antioxidant results are in good agreement with the relatively facile oxidation of dihydroacridines of groups **1** and **3**. Antioxidant compounds can act as reducing agents and, in solutions, they tend to be easily oxidized on inert electrodes. Indeed, cyclic voltammetry data indicate that compounds of groups **1** and **3** are relatively easily oxidized and characterized by well-defined peaks of irreversible oxidations [55, 56]. Low oxidation potentials (about 0.65 V versus $Ag/AgNO_3$ in acetonitrile) are associated with the ability of the dihydroacridine system to donate electron(s) and, thus, to act as antioxidants.

3. Conclusions

Our studies of the esterase profiles and estimation of antioxidant activities performed for 4 groups of acridine derivatives demonstrated that 9-aryl(hetaryl)-N-methyl-9,10-dihydroacridines (compounds **1a-j**) exhibit a high radical-scavenging activity (at the level of Trolox) and have low inhibitory potencies against AChE and BChE, while 9-aryl(hetaryl)-N-methyl-acridinium tetrafluoroborates (compounds **2a-m**) proved to be effective inhibitors of cholinesterases but lacking in antiradical activity. However, 9-Heterocyclic amino- N-methyl-9,10-dihydroacridines (compounds **3a-f**), combine effective inhibition of AChE and BChE with rather high radical-scavenging activity. Results of molecular docking well explain the observed features in the efficacy, selectivity, and mechanism of cholinesterase inhibition by the acridine derivatives. Thus, effective inhibitors of cholinesterases possessing radical scavenging capability were found in a series of acridine derivatives, thereby demonstrating that the acridine scaffold is a promising starting point for the development of multifunctional therapeutics against AD and perhaps other neurodegenerative diseases.

4. Experimental section

4.1. Synthesis of compounds

All compounds were synthesized according to established procedures already well documented in the literature [55, 56, 58, 71].

4.2. Biological assay

4.2.1. In vitro AChE, BChE, and CaE inhibition

Acetylcholinesterase (AChE, EC 3.1.1.7, from human erythrocyte), butyrylcholinesterase (BChE, EC 3.1.1.8, from equine serum), carboxylesterase (CaE, EC 3.1.1.1, from porcine liver), acetylthiocholine iodide (ATCh), butylthiocholine iodide (BTCh), 5,5´-dithiobis-(2-nitrobenzoic acid) (DTNB), and 4-nitrophenol acetate (4-NPA), were purchased from Sigma-Aldrich (Germany).

The AChE and BChE activities were measured by the Ellman method as described earlier [72]. The assay solution consisted of 0.1 M K/Na phosphate buffer (pH 7.5, 25°C) with the addition of 0.33 mM DTNB, 0.02 unit/mL of AChE or BChE, and 1 mM of substrate (ATCh or BTCh, respectively). The assays were carried out with a reagent blank containing all components except

AChE or BChE in order to account for non-enzymatic hydrolysis of substrate. In addition, an enzyme blank was included that contained all components except substrate to account for non-substrate sulfhydryl groups.

The activity of CaE was determined spectrophotometrically by the release of 4-nitrophenol at 405 nm [73]. The assay solution consisted of 0.1 M K/Na phosphate buffer (pH 8.0, 25°C) with the addition of 1 mM 4-nitrophenyl acetate and 0.02 unit/mL of CaE. The assays were carried out with a blank containing all components except CaE.

The test compounds were dissolved in DMSO; the incubation mixture contained 2% (v/v) of the solvent, a concentration determined not to affect the activity of each enzyme on its own (data not shown). The primary evaluation of inhibitory activity of compounds was carried out by determining the degree of inhibition of enzymes at a 20 μM concentration of test compound. For this, the enzyme of interest was incubated with a test compound for 10 min, and then the residual activity of the enzyme was measured. Each experiment was carried out in triplicate.

The IC_{50} values, a concentration of the inhibitor required to decrease enzyme activity by 50%, were determined for the most active compounds. To determine the IC_{50} of the inhibition of AChE and BChE, a sample of the corresponding enzyme was incubated with eight different concentrations of the test compounds in the range of 10^{-11}-10^{-4} M. Inhibitor concentrations were selected in order to obtain enzyme inhibitions of 20% to 80% of control. The test compounds were added to the assay solution and pre-incubated at 25°C with the enzymes for 10 min followed by the addition of the substrate. A parallel control was made for the assay solution with no inhibitor. Absorbance measurements were carried out using a BioRad Benchmark Plus microplate spectrophotometer (France). Each experiment was performed in triplicate. The results were expressed as the mean ± SEM calculated with GraphPad Prism 6.05 software for Windows. The reaction rates in the presence and absence of inhibitor were compared, and the percentage of residual enzyme activity due to the presence of test compounds was calculated. The IC_{50} values were determined graphically from inhibition curves (log inhibitor concentration vs. percentage of residual enzyme activity) using Origin 6.1 software for Windows.

4.2.2. Kinetic analysis of AChE and BChE inhibition. Determination of steady-state inhibition constants

To elucidate the inhibition mechanisms for the active compounds, the AChE and BChE residual activities were determined in the presence of 3 increasing concentrations of the test compounds and 6 decreasing concentrations of the substrates. The test compounds were pre-incubated with the enzymes at 25°C for 10 min, followed by the addition of the substrates. Parallel controls were made to find the rate of hydrolysis of the same concentrations of substrates in the solutions with no inhibitor. The kinetic parameters of substrate hydrolysis were determined. The measurements were carried out using a BioRad Benchmark Plus microplate spectrophotometer (France). Each experiment was performed in triplicate. The results were fitted into Lineweaver-Burk double-reciprocal kinetic plots of 1/V versus 1/[S] and the values of inhibition constants K_i (competitive component) and αK_i (noncompetitive component) were calculated using Origin 6.1 software for Windows.

4.2.3. ABTS radical cation scavenging activity assay

Radical scavenging activity of the test compounds was assessed using an $ABTS^{\cdot+}$ radical decolorization assay [66] with some modifications as described below.

ABTS (2,2′-azino-bis-(3-ethylbenzothiazoline-6-sulfonic acid) diammonium salt) was purchased from TCI (Tokyo, Japan). Potassium persulfate (di-potassium peroxodisulfate), Trolox® (6-hydroxy-2,5,7,8-tetramethychroman-2-carboxylic acid, and ascorbic acid were obtained from Sigma-Aldrich (St. Louis, MO, USA). Ethanol was HPLC grade. Aqueous solutions were prepared using deionized water.

Trolox was used as the antioxidant standard. A 5 mM solution of Trolox was prepared in DMSO for use as the stock. Fresh working solutions of standard Trolox concentrations (1-100 μM) were prepared on the day of experiments and used for calibration as well as positive controls for $ABTS^{\bullet+}$ scavenging activity.

ABTS was dissolved in deionized water to a 7 mM concentration. The solution of ABTS radical cation ($ABTS^{\cdot+}$) was produced by mixing 7 mM ABTS stock solution with 2.45 mM potassium persulfate aqueous solution in equal quantities and allowing them to react for 12–16 h at room temperature in the dark. At the time of activity, $ABTS^{\cdot+}$ solution was diluted with ethanol to adjust the absorbance value to 0.80 ± 0.02 at 734 nm. Fresh working $ABTS^{\cdot+}$ solution was prepared for each assay.

The radical scavenging capacity of the test compounds was analyzed by mixing 10 µl of compound with 240 µl of $ABTS^{\cdot+}$ working solution. The decrease in absorbance was measured spectrophotometrically at 734 nm after 1 h of mixing the solutions using a microplate UV/VIS spectrophotometer BioRad xMark (Japan). Ethanol blanks were run in each assay. Values were obtained from three replicates of each sample and three independent experiments.

The antioxidant activity was reported as Trolox equivalent antioxidant capacity (TEAC) values by comparing (A_0–A_{test}) of the test antioxidant with (A_0–A_{Trolox}) of the Trolox standard at aconcentration of 20 µM after reaction time of 1 h, where A_0 is the absorbance of a control lacking any radical scavenger, A_{test} is the absorbance of the remaining $ABTS^{\cdot+}$ in the presence of the test compound, and A_{Trolox} is is the absorbance of the remaining $ABTS^{\cdot+}$ in the presence of Trolox:

$$TEAC = (A_0–A_{test})/(A_0–A_{Trolox}).$$

For the most active compounds, we also determined the IC_{50} values (test compound concentration required for 50% reduction of the ABTS radical). The IC_{50} values were calculated using Origin 6.1 for Windows.

4.2.4. Molecular modeling

4.2.4.1. Ligand and protein structure preparation

To determine the protonation state of ionizable groups of the compounds, Marvin 14.9.1.0 (ChemAxon, http://www.chemaxon.com) was used to estimate pK_a values. Geometries of the ligands were quantum-mechanically (QM) optimized in the Gamess-US package [74] using DFT method B3LYP and basis set 6-31G*. Partial atomic charges were taken from QM results according to the Mulliken scheme [75]. These optimized geometries and partial charges were used for molecular docking.

For AChE, there are several structures available in the Protein Data Bank (PDB) of the human enzyme (hAChE) in the apo state or in complex with several ligands (PDB ID 4EY4-4EY8, [76]). All X-ray structures as well as the water-saturated structure of apo-hAChE optimized with molecular mechanics (MM) were used for molecular docking as described previously [64]. Similar to results obtained in [64], the best binding affinities were obtained with structure PDB ID 4EY7 (hAChE co-crystallized with Donepezil, resolution = 2.35Å) and were comparable to results obtained with the water-saturated MM-optimized structure of apo-hAChE.

For BChE, the X-ray structure of the human enzyme (PDB ID 1P0I [77]) was used. Previously, the importance of saturation of the BChE gorge with water molecules was demonstrated [78]. Consequently, the structure was saturated with water molecules and optimized using a QM/MM method as reported previously [78, 79].

4.2.4.2. Molecular docking

Molecular docking with a Lamarckian Genetic Algorithm (LGA) [80] was performed using Autodock 4.2.6 [81] and AutoDock Vina 1.1.2 [82] software. The rectangular prism grid box for docking included the whole active site and the gorge of AChE (22.5 Å×22.5 Å×22.5 Å grid box dimensions) and BChE (15Å × 20.25Å × 18Å grid box dimensions) with grid spacing of 0.375 Å. The main selected LGA parameters were 256 runs, 25×10^6 evaluations, 27×10^4 generations and population size of 300. For AutoDock Vina the same grid boxes were used along with an exhuastiveness setting of 40. Autodock Vina results were in very good agreement. Structural images were prepared with PyMOL (Schrödinger, LLC).

Acknowledgements

This work was partly supported by grant No 17-03-00984 of the Russian Foundation for Basic Research and program "Medicinal Chemistry" of the Russian Academy of Sciences. We thank the Lomonosov Supercomputer center [83] for computational time. We are also grateful to the Center of the Collective-Access Equipment of the Institute of Physiologically Active Compounds, Russian Academy of Sciences for use of equipment (agreement no. 14.621.21.0008, ID no. RFMEFI62114X0008). The funding sources had no role in the study design; collection, analysis and interpretation of data; writing of the manuscript; or the decision to submit the article for publication.

References

1. Bongarzone S, Bolognesi ML *Expert Opin Drug Discov.* 2011;6:251. doi:10.1517/17460441.2011.550914

2. Wainwright M *J Antimicrob Chemother.* 2001;47:1. doi:10.1093/jac/47.1.1

3. Girault S, Grellier P, Berecibar A, et al. *J Med Chem.* 2000;43:2646. doi:10.1021/jm990946n

4. Gamage SA, Figgitt DP, Wojcik SJ, et al. *J Med Chem.* 1997;40:2634. doi:10.1021/jm970232h

5. Lyakhov SA, Suveyzdis YI, Litvinova LA, et al. *Pharmazie* 2000;55:733.

6. Denny WA *Curr Med Chem.* 2002;9. doi:10.2174/0929867023369277

7. Korth C, May BC, Cohen FE, Prusiner SB *Proc Natl Acad Sci USA.* 2001;98:9836. doi:10.1073/pnas.161274798

8. Collinge J, Gorham M, Hudson F, et al. *Lancet Neurol.* 2009;8:334. doi:10.1016/s1474-4422(09)70049-3

9. Klingenstein R, Lober S, Kujala P, et al. *J Neurochem.* 2006;98:748. doi:10.1111/j.1471-4159.2006.03889.x

10. Sondhi SM, Singh J, Rani R, et al. *Eur J Med Chem.* 2010;45:555. doi:10.1016/j.ejmech.2009.10.042

11. Mallu L, Thirumalai D, Asharani IV *Chem Biol Drug Des.* 2017. doi:10.1111/cbdd.12973

12. Lermontova N, Lukoyanov N, Serkova T, et al. *Molecular and Chemical Neuropathology.* 1998;33:51. doi:10.1007/bf02815859

13. Csuk R, Barthel A, Raschke C, et al. *Arch Pharm (Weinheim).* 2009;342:699. doi:10.1002/ardp.200900065

14. Antosova A, Chelli B, Bystrenova E, et al. *Biochim Biophys Acta.* 2011;1810:465. doi:10.1016/j.bbagen.2011.01.007

15. Prasad A, Raju G, Sivalingam V, et al. *Sci Rep.* 2016;6:39490. doi:10.1038/srep39490

16. Mufson EJ, Counts SE, Perez SE, Ginsberg SD *Expert Rev Neurother.* 2008;8:1703. doi:10.1586/14737175.8.11.1703

17. Martinez A, Castro A *Expert Opin Investig Drugs.* 2006;15:1. doi:10.1517/13543784.15.1.1

18. Mesulam MM, Guillozet A, Shaw P, et al. *Neurosci.* 2002;110:627. doi:10.1016/s0306-4522(01)00613-3

19. Ballard C, Greig N, Guillozet-Bongaarts A, et al. *Curr Alzheimer Res.* 2005;2:307. doi:10.2174/1567205054367838

20. Greig NH, Utsuki T, Ingram DK, et al. *Proc Natl Acad Sci USA.* 2005;102:17213. doi:10.1073/pnas.0508575102

21. Lane RM, Potkin SG, Enz A *Int J Neuropsychopharmacol.* 2006;9:101. doi:10.1017/S1461145705005833

22. Macdonald IR, Rockwood K, Martin E, Darvesh S *J Alzheimers Dis.* 2014;42:379. doi:10.3233/JAD-140219

23. Klafki HW, Staufenbiel M, Kornhuber J, Wiltfang J *Brain.* 2006;129:2840. doi:10.1093/brain/awl280

24. Mangialasche F, Solomon A, Winblad B, et al. *Lancet Neurol.* 2010;9:702. doi:10.1016/S1474-4422(10)70119-8

25. Carreiras MC, Mendes E, Perry MJ, et al. *Curr Top Med Chem.* 2013;13:1745. doi:10.2174/15680266113139990135

26. Bachurin SO, Bovina EV, Ustyugov AA *Med Res Rev.* 2017;37:1186. doi:10.1002/med.21434

27. Markesbery WR *Free Radic Biol Med.* 1997;23:134. doi:10.1016/s0891-5849(96)00629-6

28. Ortiz GG, Pacheco Moisés FP, Mireles-Ramírez M, et al., Oxidative Stress: Love and Hate History in Central Nervous System, Advances in Protein Chemistry and Structural Biology, Academic Press2017.

29. Moreira PI, Siedlak SL, Aliev G, et al. *J Neural Transm (Vienna).* 2005;112:921. doi:10.1007/s00702-004-0242-8

30. Rosini M, Simoni E, Bartolini M, et al. *Eur J Med Chem.* 2011;46:5435. doi:10.1016/j.ejmech.2011.09.001

31. Guzior N, Wieckowska A, Panek D, Malawska B *Curr Med Chem.* 2015;22:373. doi:10.2174/0929867321666141106122628

32. Oztaskin N, Cetinkaya Y, Taslimi P, et al. *Bioorg Chem.* 2015;60:49. doi:10.1016/j.bioorg.2015.04.006

33. Dudai Y, Silman I, Shinitzky M, Blumberg S *Proc Natl Acad Sci USA.* 1972;69:2400.

34. Kozurkova M, Hamulakova S, Gazova Z, et al. *Pharmaceuticals.* 2011;4:382. doi:10.3390/ph4020382

35. Jin H *Med Chem.* 2014;4. doi:10.4172/2161-0444.1000213

36. Crismon ML *Ann Pharmacother.* 1994;28:744. doi:10.1177/106002809402800612

37. Watkins PB *JAMA.* 1994;271:992. doi:10.1001/jama.1994.03510370044030

38. Tumiatti V, Minarini A, Bolognesi ML, et al. *Curr Med Chem.* 2010;17:1825.

39. Romero A, Cacabelos R, Oset-Gasque MJ, et al. *Bioorg Med Chem Lett.* 2013;23:1916. doi:10.1016/j.bmcl.2013.02.017

40. Minarini A, Milelli A, Simoni E, et al. *Curr Top Med Chem.* 2013;13:1771. doi:10.2174/15680266113139990136

41. A.N. de Aquino R, V. Modolo L, B. Alves R, de Fatima A *Curr Drug Targets.* 2013;14:378. doi:10.2174/1389450111314030010

42. Imai T *Drug Metab Pharmacokinet.* 2006;21:173. doi:10.2133/dmpk.21.173

43. Laizure SC, Herring V, Hu Z, et al. *Pharmacotherapy.* 2013;33:210. doi:10.1002/phar.1194

44. Tsurkan LG, Hatfield MJ, Edwards CC, et al. *Chem Biol Interact.* 2013;203:226. doi:10.1016/j.cbi.2012.10.018

45. Cain BF, Seelye RN, Atwell GJ *J Med Chem.* 1974;17:922. doi:10.1021/jm00255a003

46. Albert A, The Acridines, Edward Arnold Ltd., London, 1966.

47. Liu Z, Dong N, Xu M, et al. *J Org Chem.* 2013;78:7436. doi:10.1021/jo400803s

48. Charushin VN, Chupakhin ON *Pure Appl Chem.* 2004;76. doi:10.1351/pac200476091621

49. Makosza M *Chem Soc Rev.* 2010;39:2855. doi:10.1039/b822559c

50. Mąkosza M *Synthesis.* 2011;2011:2341. doi:10.1055/s-0030-1260668

51. Mąkosza M, Wojciechowski K *Heterocycles.* 2014;88:75. doi:10.3987/rev-13-sr(s)1

52. Terrier F, Modern Nucleophilic Aromatic Substitution, Wiley-VCH, Weinheim, 2013.

53. Chen Q, Leon T, Knochel P *Angew Chem Int Ed Engl.* 2014;53:8746. doi:10.1002/anie.201400750

54. Chupakhin ON, Charushin VN, van der Plas HC, Nucleophilic Aromatic Substitution of Hydrogen, Academic Press, New York, San Diego, 1994.

55. Shchepochkin AV, Chupakhin ON, Charushin VN, et al. *RSC Adv.* 2016;6:77834. doi:10.1039/c6ra17783b

56. Shchepochkin AV, Chupakhin ON, Charushin VN, et al. *Russ Chem Bull.* 2014;62:773. doi:10.1007/s11172-013-0105-2

57. Chupakhin ON, Shchepochkin AV, Charushin VN *Green Chem.* 2017;19:2931. DOI: 10.1039/c7gc00789b . doi:10.1039/c7gc00789b

58. Chupakhin ON, Charushin VN, Shchepochkin AV, 2016133839, 2016.

59. Makhaeva GF, Radchenko EV, Baskin, II, et al. *SAR QSAR Environ Res.* 2012;23:627. doi:10.1080/1062936X.2012.679690

60. Makhaeva GF, Radchenko EV, Palyulin VA, et al. *Chem Biol Interact.* 2013;203:231. doi:10.1016/j.cbi.2012.10.012

61. Makhaeva GF, Lushchekina SV, Boltneva NP, et al. *Sci Rep.* 2015;5:13164. doi:10.1038/srep13164

62. Makhaeva GF, Rudakova EV, Serebryakova OG, et al. *Chem Biol Interact.* 2016;259(Pt B):332. doi:10.1016/j.cbi.2016.05.002

63. Makhaeva GF, Boltneva NP, Lushchekina SV, et al. *Bioorg Med Chem.* 2016;24:1050. doi:10.1016/j.bmc.2016.01.031

64. Semenov VE, Zueva IV, Mukhamedyarov MA, et al. *ChemMedChem.* 2015;10:1863. doi:10.1002/cmdc.201500334

65. Kharlamova AD, Lushchekina SV, Petrov KA, et al. *Biochem J.* 2016;473:1225. doi:10.1042/BCJ20160084

66. Re R, Pellegrini N, Proteggente A, et al. *Free Radic Biol Med.* 1999;26:1231. doi:10.1016/s0891-5849(98)00315-3

67. Craft BD, Kerrihard AL, Amarowicz R, Pegg RB *Compr Rev Food Sci Food Saf.* 2012;11:148. doi:10.1111/j.1541-4337.2011.00173.x

68. Shahidi F, Wanasundara PK *Crit Rev Food Sci Nutr.* 1992;32:67. doi:10.1080/10408399209527581

69. Jung J, Ohkubo K, Goldberg DP, Fukuzumi S *J Phys Chem A.* 2014;118:6223. doi:10.1021/jp505860f

70. Matern AI, Charushin VN, Chupakhin ON *Russ Chem Rev.* 2007;76:23. doi:10.1070/RC2007v076n01ABEH003647

71. Chupakhin ON, Charushin VN, Shchepochkin AV, Patent RU 2582126, 2016.

72. Ellman GL, Courtney KD, Andres V, Jr., Feather-Stone RM *Biochem Pharmacol.* 1961;7:88. doi:10.1016/0006-2952(61)90145-9

73. Sterri SH, Johnsen BA, Fonnum F *Biochem Pharmacol.* 1985;34:2779. doi:10.1016/0006-2952(85)90579-9

74. Schmidt MW, Baldridge KK, Boatz JA, et al. *J Comput Chem.* 1993;14:1347. doi:10.1002/jcc.540141112

75. Mulliken RS *J Chem Phys.* 1955;23:1841. doi:10.1063/1.1740588

76. Cheung J, Rudolph MJ, Burshteyn F, et al. *J Med Chem.* 2012;55:10282. doi:10.1021/jm300871x

77. Nicolet Y, Lockridge O, Masson P, et al. *J Biol Chem.* 2003;278:41141. doi:10.1074/jbc.M210241200

78. Masson P, Lushchekina S, Schopfer LM, Lockridge O *Biochem J.* 2013;454:387. doi:10.1042/BJ20130389

79. Lushchekina SV, Polomskikh VS, Varfolomeev SD, Masson P *Russ Chem Bull.* 2013;62:2527. doi:10.1007/s11172-013-0366-9

80. Morris GM, Goodsell DS, Halliday RS, et al. *J Comput Chem.* 1999;19:1639. doi:10.1002/(SICI)1096-987X(19981115)19:14<1639::AID-JCC10>3.0.CO;2-B

81. Morris GM, Huey R, Lindstrom W, et al. *J Comput Chem.* 2009;30:2785. doi:10.1002/jcc.21256

82. Trott O, Olson AJ *J Comput Chem.* 2010;31:455. doi:10.1002/jcc.21334

83. Sadovnichy V, Tikhonravov A, Voevodin V, Opanasenko V, "Lomonosov": supercomputing at Moscow State University, in: J.S. Vetter (Ed.) Contemporary High Performance Computing: From Petascale toward Exascale, CRC Press, Boca Raton, USA, 2013, pp. 283.

Highlights

- 9-aryl-N-methyl-9,10-dihydroacridines (9-aryl-NMDHAs) are radical scavengers
- 9-aryl-N-methyl-acridinium tetrafluoroborates are cholinesterase inhibitors.
- 9-heterocyclic amino-NMDHAs are radical scavengers and cholinesterase inhibitors.

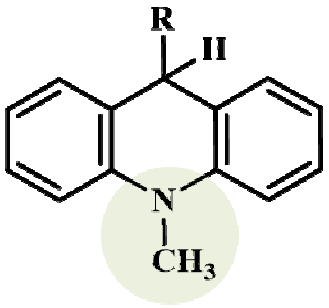

Antioxidants

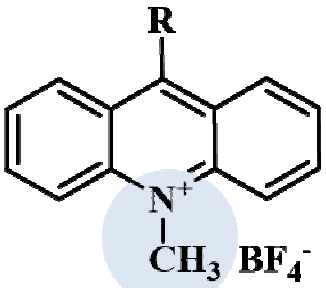

Cholinesterase inhibitors

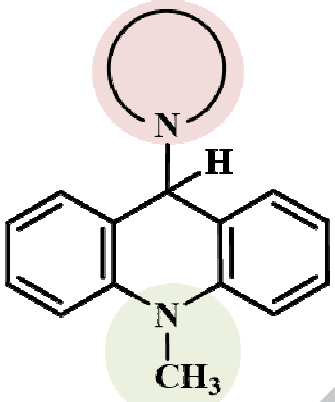

Cholinesterase inhibitors
&
Antioxidants